USGS
science for a changing world

Prepared for the National Aeronautics and Space Administration

Geologic Map of the Meskhent Tessera Quadrangle (V–3), Venus

By Mikhail A. Ivanov and James W. Head, III

Pamphlet to accompany
Scientific Investigations Map 3018

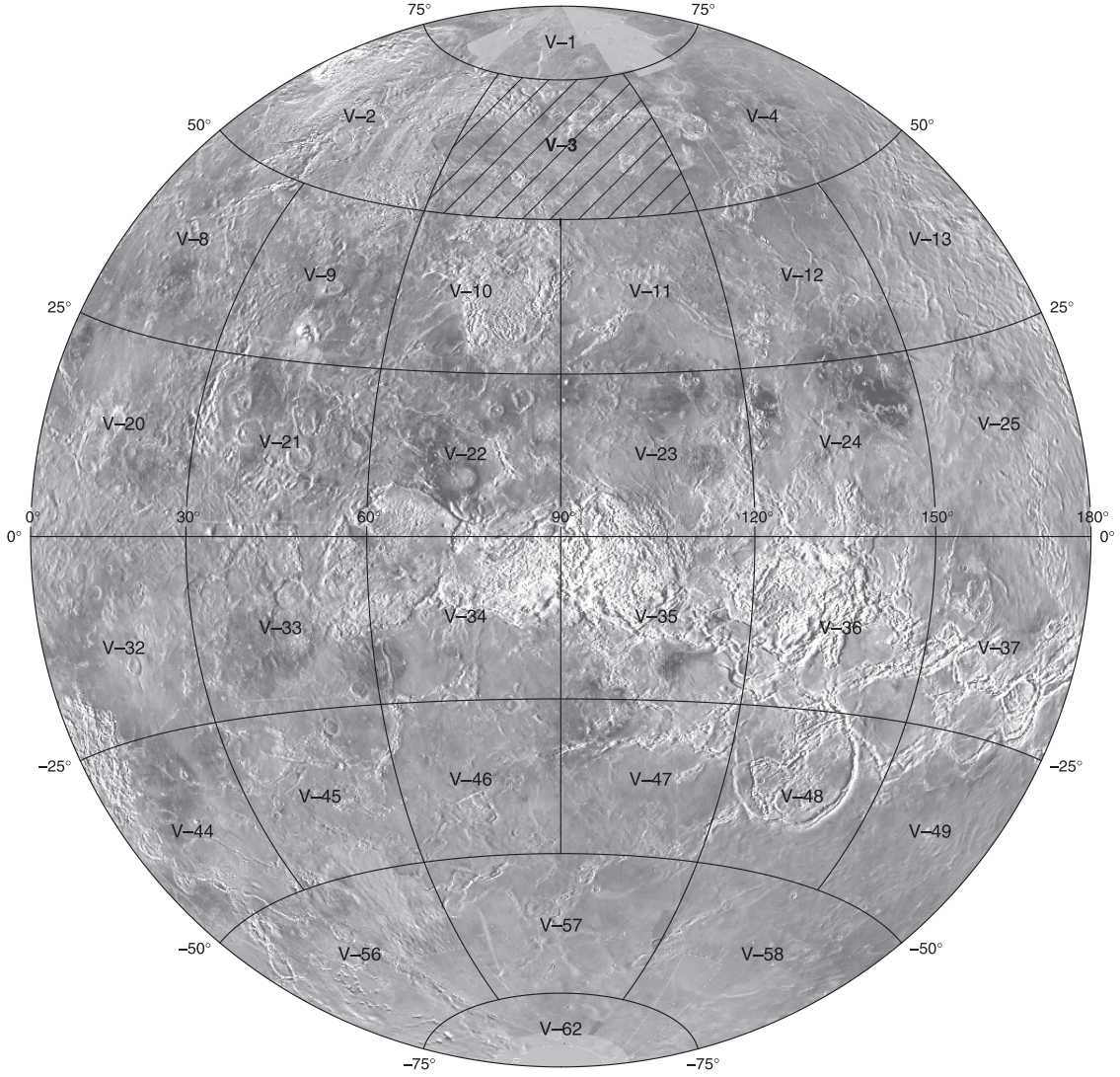

2008

U.S. Department of the Interior
U.S. Geological Survey

The Magellan Mission

The Magellan spacecraft orbited Venus from August 10, 1990, until it plunged into the Venusian atmosphere on October 12, 1994. Magellan Mission objectives included (1) improving the knowledge of the geological processes, surface properties, and geologic history of Venus by analysis of surface radar characteristics, topography, and morphology and (2) improving the knowledge of the geophysics of Venus by analysis of Venusian gravity.

The Magellan spacecraft carried a 12.6-cm radar system to map the surface of Venus. The transmitter and receiver systems were used to collect three data sets: (1) synthetic aperture radar (SAR) images of the surface, (2) passive microwave thermal emission observations, and (3) measurements of the backscattered power at small angles of incidence, which were processed to yield altimetric data. Radar imaging and altimetric and radiometric mapping of the Venusian surface were accomplished in mission cycles 1, 2, and 3 from September 1990 until September 1992. Ninety-eight percent of the surface was mapped with radar resolution on the order of 120 m. The SAR observations were projected to a 75-m nominal horizontal resolution, and these full-resolution data compose the image base used in geologic mapping. The primary polarization mode was horizontal-transmit, horizontal-receive (HH), but additional data for selected areas were collected for the vertical polarization sense. Incidence angles varied between about 20° and 45°.

High-resolution Doppler tracking of the spacecraft took place from September 1992 through October 1994 (mission cycles 4, 5, 6). Approximately 950 orbits of high-resolution gravity observations were obtained between September 1992 and May 1993 while Magellan was in an elliptical orbit with a periapsis near 175 km and an apoapsis near 8,000 km. An additional 1,500 orbits were obtained following orbit-circularization in mid-1993. These data exist as a 75° by 75° harmonic field.

Magellan Radar Data

Radar backscatter power is determined by (1) the morphology of the surface at a broad range of scales and (2) the intrinsic reflectivity, or dielectric constant, of the material. Topography at scales of several meters and larger can produce quasi-specular echoes, and the strength of the return is greatest when the local surface is perpendicular to the incident beam. This type of scattering is most important at very small angles of incidence, because natural surfaces generally have few large tilted facets at high angles. The exception is in areas of steep slopes, such as ridges or rift zones, where favorably tilted terrain can produce very bright signatures in the radar image. For most other areas, diffuse echoes from roughness at scales comparable to the radar wavelength are responsible for variations in the SAR return. In either case, the echo strength is also modulated by the reflectivity of the surface material. The density of the upper few wavelengths of the surface can have a significant effect. Low-density layers, such as crater ejecta or volcanic ash, can absorb the incident energy and produce a lower observed echo. On Venus, a rapid increase in reflectivity exists at a certain critical elevation above which high-dielectric minerals or coatings are thought to be present. This leads to very bright SAR echoes from virtually all areas above that critical elevation.

The measurements of passive thermal emission from Venus, though of much lower spatial resolution than the SAR data, are more sensitive to changes in the dielectric constant of the surface than to roughness. They can be used to augment studies of the surface and to discriminate between roughness and reflectivity effects. Observations of the near-nadir backscatter power, collected using a separate smaller antenna on the spacecraft, were modeled using the Hagfors expression for echoes from gently undulating surfaces to yield estimates of planetary radius, Fresnel reflectivity, and root-mean-square (rms) slope. The topographic data produced by this technique have horizontal footprint sizes of about 10 km near periapsis and a vertical resolution on the order of 100 m. The Fresnel reflectivity data provide a comparison to the emissivity maps, and the rms slope parameter is an indicator of the surface tilts, which contribute to the quasi-specular scattering component.

Introduction

The Meskhent Tessera quadrangle (V–3, fig. 1) is in the northern hemisphere of Venus and extends from lat 50° to 75° N. and from long 60° to 120° E. In regional context, the Meskhent Tessera quadrangle is surrounded by extensive tessera regions to the west (Fortuna and Laima Tesserae) and to the south (Tellus Tessera) (Sukhanov, 1992) and by a large basin-like lowland (Atalanta Planitia) on the east (Ivanov and Head, 2004a). The northern third of the quadrangle (fig. 2a) covers the easternmost portion of the large topographic province of Ishtar Terra (northwestern map area) and the more localized upland of Tethus Regio (northeastern map area). Both eastern Ishtar Terra and Tethus Regio are outlined by the 1-km-contour line but the surface of Ishtar reaches an elevation about 3–3.5 km above mean planetary radius; the majority of Tethus Regio is between 1–2 km elevation (fig. 2b). The majority of the quadrangle lies within the midland topographic province (0–2 km above mean planetary radius, Masursky and others, 1980; Pettengill and others, 1980; Ivanov and Head, 2004c).

Before the Magellan mission, the geology of the Meskhent Tessera quadrangle was mapped from topographic data acquired by the Pioneer-Venus altimeter (Masursky and others, 1980; Pettengill and others, 1980) and radar images received by the Soviet Venera-15/16 mission (Barsukov and others, 1986; Sukhanov and others, 1989). Venera-15/16 radar images showed that several large massifs of tessera terrain, corresponding to elevated regions, occupied the periphery of the map area. Some coronae and coronalike features (Pronin and Stofan, 1990; Stofan and Head, 1990) and riftlike fracture zones occur within the low-lying areas between tessera massifs. Venera-15/16 data further revealed that the central and southern map area were characterized by complex patterns of features such as deformational belts and volcanic plains (Sukhanov and others, 1989). A few distinct, large volcanic centers to the north and south of

Tethus Regio appeared to be the sources of outpourings of digitate lava flows down the regional slopes of Tethus.

Early Magellan results revealed that the interior of the map area was populated with complex patterns of deformational features in the form of belts of ridges and grooves (Solomon and others, 1992). The most prominent belt of ridges is Allat Dorsa that runs along the north edge of Dekla Tessera in the southwest corner of the map area. An extensive zone of fractures and graben (Manto Fossae) occurs in the west-central portion of the quadrangle between Dekla Tessera to the south and eastern Ishtar Terra (Fortuna Tessera) to the north. Dispersed fragments of both ridge and groove belts occur throughout the map area. Global analysis of the distribution of volcanic features revealed that the map area is relatively deficient in distinctive large volcanic centers, except for three coronae and two volcanoes (Head and others, 1992; Crumpler and others, 1993; Crumpler and Aubele, 2000), but that it is densely populated by small shieldlike and conelike features a few kilometers across that are interpreted to be volcanic edifices (Crumpler and Aubele, 2000; Ivanov and Head, 2004b).

Our primary focus for geological study in the Meskhent quadrangle is the transition zone from uplands to lowlands. The gravity characteristics (Bindschadler and others, 1992b; Konopliv and Sjogren, 1994; Konopliv and others, 1999) and topography of Atalanta Planitia to the east of the map area have been cited as evidence for the region being the site of large-scale mantle downwelling (Bindschadler and others, 1992b). The topographic configuration, gravity signature, and presence of large tesserae in Ishtar Terra, Tethus Regio, and Tellus Tessera are consistent with extensive areas of thickened crust and tectonically stabilized lithosphere that represent ancient and possibly now extinct regimes of mantle convection (Grimm, 1994; Brown and Grimm, 1999). Thus, the region of Meskhent Tessera quadrangle represents a good sample for the study of several major processes on Venus: (1) the formation and evolution of lowlands, midlands, and highlands, (2) the interaction between mantle downwelling and areas of thickened crust and lithosphere, (3) the formation of associated tectonic features, and (4) the emplacement of volcanic plains. The major questions and issues are addressed by geological mapping in the Meskhent Tessera quadrangle and provide the basis for our mapping analysis: What is the sequence of events in the formation and evolution of large-scale lowlands and uplands on Venus? What are the characteristics of the marginal areas of midlands surrounding these topographic provinces? How did the transition zone of midlands from the uplands of Ishtar Terra and Tethus Regio to the lowland of Atalanta Planitia evolve? What information do the units in Meskhent Tessera quadrangle provide concerning models for Venus global stratigraphy and tectonic history?

In our analysis, we have focused on the geologic mapping of the Meskhent Tessera quadrangle using traditional methods of geologic unit definition and characterization for the Earth (for example, American Commission on Stratigraphic Nomenclature, 1961; North American Commission on Stratigraphic Nomenclature, 1983) and the planets (for example, Wilhelms, 1990) appropriately modified for radar data (Tanaka, 1994). We defined units and mapped key relations using the full-resolution Magellan SAR data (mosaicked full-resolution basic image data records, C1-MIDRs, F-MIDRs, and F-Maps) and transferred these results to the base map compiled at a scale of 1:5,000,000. In addition to the SAR image data, we incorporated into our analyses digital versions of Magellan altimetry, emissivity, Fresnel reflectivity, and roughness data (rms slope). The background for our unit definition and characterization is described in Tanaka (1994), Basilevsky and Head (1995a,b), Basilevsky and others (1997), and Ivanov and Head (1998, 2001a,b) and further discussed in Hansen (2000) and Basilevsky and Head (1998, 2000).

Magellan Sar and Related Data

The SAR instrument flown on the Magellan spacecraft (12.6 cm, S-band) provided the image data used in this mapping and interpretation. SAR images are a record of the echo (radar energy returned to the antenna), which is influenced by surface composition, slope, and wavelength-scale surface roughness. Viewing and illumination geometry also influence the appearance of surface features in SAR images. Guidelines for geologic mapping using Magellan SAR images and detailed background to aid in their interpretation can be found in Elachi (1987), Saunders and others (1992), Ford and Pettengill (1992), Tyler and others (1992), and Tanaka (1994). In the area of the Meskhent Tessera quadrangle, incidence angles (16.3–21.3 for Cycle 1 and 19.7–25.1 for Cycle 2; Ford and others, 1993) show that backscatter is dominated by variations in surface roughness at wavelength scales. Rough surfaces appear relatively bright, whereas, smooth surfaces appear relatively dark. Variations also occur depending on the orientation of features relative to the incident radiation (illumination direction); features normal to the illumination direction are more prominent than those oriented parallel to it. Full-resolution images have a pixel size of 75 m; C1-MIDRs contain the SAR data displayed at approximately 225 m/pixel. Altimetry data and stereo images were of extreme importance in establishing geologic and stratigraphic relations between units. Data obtained by Magellan on the emissivity (passive thermal radiation), reflectivity (surface electrical properties), and rms slope (distribution of radar wavelength scale slopes) are also essential in the analysis of the geology of the surface. Aspects of these measurements were used in unit characterization and interpretation; background on the characteristics of these data and their interpretation may be found in Saunders and others (1992), Ford and Pettengill (1992), Tyler and others (1992), Tanaka (1994), and Campbell (1995).

General Geology

Several different geologic processes have influenced the Meskhent Tessera region and have combined to form its geologic record. Volcanism is apparently the dominant process of crustal formation on Venus (Head and others, 1992), and it produced the observed material units in the map area. A variety of volcanic and volcano-tectonic features that occur within the quadrangle is listed in table 1. Tectonic activity has modified

some of these basic crustal materials (for example, Solomon and others, 1992; Squyres and others, 1992) in a variety of modes (extension and contraction). In places such as tessera, ridge belts, and groove belts, deformation is so dense that the underlying material unit is obscured and deformational features become part of the definition of the material unit (see also Tanaka, 1994; Scott and Tanaka, 1986). Impact cratering (table 2) has also locally influenced regions in the quadrangle but generally has not been an influential process throughout the map area. Aeolian processes require a source of sediment to produce deposits and, thus, are concentrated around impact craters (for instance, crater La Fayette) and localized around tectonic fractures and scarps (for example, Greeley and others, 1992).

The area of the Meskhent Tessera quadrangle displays three major occurrences of tessera (fig. 3), where several tectonic styles have developed together or in sequence to produce terrain that is more heavily deformed than typical regional plains and where the deformation is so intense that it becomes a major part of the unit definition (for example, Bindschadler and others, 1992a). The largest occurrence of tessera terrain occurs in the northwestern map area and corresponds to the eastern extension of Fortuna Tessera that occupies a significant part of Ishtar Terra to the west of the quadrangle. An elongated tessera massif (Meskhent Tessera, about 1,300 km long and 300–350 km wide; Raitala, 1996) is in the central portion of Tethus Regio, and an arclike zone of tessera terrain (Dekla Tessera) occurs in the southwest corner of the quadrangle. Smaller outliers of tessera (tens to a few hundreds of kilometers across) typically occur near the major tessera regions.

Other tectonic features in the Meskhent Tessera quadrangle (fig. 3) mostly cluster in distinct deformation belts that consist of either contractional or extensional structures. In some places, however, extensional structures complicate deformational belts that predominantly consist of contractional ridges. The belts of grooves (Manto Fossae), which are about 100–150 km wide, are among the most prominent structures on the floor of the lowlands of Audra Planitia between Dekla and Fortuna Tesserae. The structural trend of these groove belts continues from the west margin to the south margin of the map area, forming a giant arc of extensional structures that is roughly parallel to the general trend of the arc of Dekla Tessera. In the southwest corner of the map area, another diffuse zone of groove belts is oriented to the northeast, almost orthogonal to orientation of the Manto Fossae zone. Another prominent zone of groove belts stretches from Fakahotu Corona to the northeast. Individual extensional features in the quadrangle include narrow (less than ~1–2 km) graben, hundreds of kilometers in length, that radiate from the area of Fakahotu Corona and a nova (radial fracture center) at about lat 69° N., long 88° E. (Crumpler and Aubele, 2000).

Dense swarms of ridges, which are typically 5–10 km wide, are collected in a ridge belt (Allat Dorsa) that is in contact with Dekla Tessera and follows the strike of this tessera arc. In the center of the quadrangle, smaller fragments of ridge belts form a semicircular feature that outlines a corona-like feature, Vacuna Corona. Fragments of ridge belts form the southern part of Fakahotu Corona and the southern and eastern portions of the rim of Tusholi Corona. Wrinkle ridges are widespread throughout the regional plains that cover most of the surface of lowlands between the major tessera occurrences. The typical length of wrinkle ridges is several tens of kilometers and width is a few kilometers. Wrinkle ridges and ridge belts are interpreted to represent contractional deformation.

In many areas of the Meskhent Tessera quadrangle, clusters of small (<15 km) domes, interpreted as shield volcanoes (Aubele and Slyuta, 1990; Guest and others, 1992; Aubele, 1994, 1995; Crumpler and Aubele, 2000; Addington, 2001; Ivanov and Head, 2004b), are common in spatial association with tessera massifs and deformation belts. Individual small shields occur relatively rarely within the vast extent of regional plains that cover the surface between the belts and within the northern portion of the map area. The small shields are low in elevation, commonly have a summit pit, do not appear to have distinct associated flows, and are commonly embayed by subsequent regional plains deposits (for example, Kreslavsky and Head, 1999; Ivanov and Head, 2001b, 2004b). Concentrations of small shield volcanoes occur throughout the quadrangle. Several steep-sided domes (Pavri and others, 1992; Ivanov and Head, 1999; Stofan and others, 2000) have been found in the Meskhent Tessera quadrangle, usually in spatial association with fields of small shields.

There are two meanings of the term “plains” (Mescherikov, 1968). In a strict morphological sense, plains define morphologically uniform surfaces with relatively small differences in relief. In a broader sense, plains are counterparts of highlands and define vast flat terrains. In the strict sense, the term “plains” is simply a descriptor of a type of surface and does not infer an interpretative meaning. At the higher level of interpretation, the term “volcanic plains” implies knowledge or inference of the nature of material that makes up the plains. On Venus, however, the materials that form plains are most likely of volcanic origin. In the broader sense, the term “plains” usually describes large physiographic provinces (for example, North American plains, Russian plain). Thus, the same term may define two different classes of morphologic/physiographic features. Although the specific meaning of the term “plains” is usually clear from the context, misunderstanding in its usage may occur. Fortunately, in planetary nomenclature, the physiographic and physiographic-topographic meanings of the term “plains” are strictly defined. A vast plainlike and more or less homogeneous physiographic province is called “planitia” if it is at middle to low elevations (for example, Atalanta Planitia or Isidis Planitia on Mars) or “planum” if it is elevated (for example Lakshmi Planum or Hesperia Planum on Mars). Following this rule, we use the term “plains” in the nongenetic, morphological sense throughout the discussion and Description of Map Units. Using specific morphologic and physical property characteristics, we define various different plains units in the unit descriptions. For example, lobate plains differ from shield plains and so on.

Several coronae occur within the quadrangle (Stofan and others, 1992, 2001; Crumpler and others, 1993; Crumpler and Aubele, 2000). Tusholi Corona and Ops Corona formed in a broad topographic trough that separates the uplands of Ishtar Terra and Tethus Regio. Fakahotu Corona, in the east-central map area, appears to represent the southwest extension of a chain of coronae interconnected by swarms of graben along the west edge of Atalanta Planitia, while Atalanta Planitia

lacks coronae (Atalanta Planitia quadrangle, V–4, Ivanov and Head, 2004a). Extensive complexes of lava flows (fluctūs) that characterize, for example, the transition between Lada Terra and Lavinia Planitia (Mylitta Fluctus quadrangle, V–61, Ivanov and Head, 2005) are absent within the map area, but digitate lava flows form a lava apron around Fakahotu Corona. Distinct flowlike features that compose the apron clearly indicate both the source regions and flow paths. The flows are almost tectonically undeformed and follow the current topography, which means that the relief in the areas of the flows did not change significantly since their emplacement. About one third of the quadrangle consists of plains of relatively homogeneous radar brightness that are interpreted to be volcanic and are modified by tectonic structures to varying, but usually low, degrees. The plains are mostly concentrated within the lower areas (Audra Planitia, Lowana Planitia, and others) that extend between the major outcrops of tessera terrain; the source vents for these volcanic plains are mostly unknown. Some of these plains display radar backscatter variations and apparent flow fronts that permit stratigraphic distinctions among subunits. The composition of the homogeneous and inhomogeneous volcanic plains is not known from data in this quadrangle, although Venera 9, 10, 13, and 14 (northeast and southeast slope of Beta Regio) and Vega 1 and 2 lander geochemical analyses of sites in similar terrains suggest compositions similar to terrestrial basalts (Basilevsky and others, 1992).

Twelve impact craters are mapped in the quadrangle (fig. 4, table 2). Crater size ranges from 4.5-km-diameter crater Miovasu to 57.6-km-diameter crater Fedorets (Herrick and others, 1997; Schaber and others, 1998, table 2). Craters La Fayette and Fedorets have outflow deposits, and craters La Fayette and Jadwiga appear to be surrounded by mantling deposits possibly emplaced during the cratering event (both outflow deposits and dark haloes; Schaber and others, 1992; Phillips and others, 1992; Campbell and others, 1992; Schultz, 1992). The spatial association of morphologically smooth and featureless plains with materials of these craters suggests that the materials (at least in part) represent degraded remnants of dark haloes (Basilevsky and others, 2003; Bondarenko and Head, 2004). Small areas near craters La Fayette and Jadwiga are apparently covered with fragmental surface materials that have been redistributed by aeolian processes. No splotches were detected in the quadrangle; splotches are interpreted to be the surface markings and deposits due to airblasts from projectiles traversing the atmosphere (for example, Schaber and others, 1992; Ivanov and others, 1992).

Stratigraphy

A crater retention age for the present surface of Venus of ~800 Ma (McKinnon and others, 1997), ~500 Ma (Schaber and others, 1992; Phillips and others, 1992), or ~300 Ma (Strom and others, 1994) has been proposed on the basis of an analysis of the global size-frequency distribution of impact craters. The crater areal distribution cannot be distinguished from a spatially random population (Hauck and others, 1998; Campbell, 1999), which, combined with the small total number of craters, means that crater size-frequency distributions cannot be used to date stratigraphic units for an area the size of the Meskhent Tessera quadrangle. Therefore, we focus on the definition of geologic units and structures and the analysis of crosscutting, embayment, and superposition relations to establish the regional geologic history.

Although we have mapped tectonic structures independently of geologic units, tectonic features are sometimes such a pervasive part of the morphology of the terrain that it is difficult to impossible to determine the nature of the underlying material, and the structure becomes part of the definition of a unit. For example, our tessera material (unit t) is analogous to Aureole member 4 of the Olympus Mons Formation on Mars ("Forms broad . . . lobes; corrugated, cut by numerous faults that formed scarps and deep troughs and grabens," Scott and Tanaka, 1986) and our ridged plains material (unit pr) is similar to ridge band material on Europa (". . . linear to curvilinear features consisting of alternating ridges and troughs . . . ," Figueredo and Greeley, 2000). In recently published Venus maps, similar unit definitions were successfully used to map quadrangles that portray geologically diverse provinces (Rosenberg and McGill, 2001; Bridges and McGill, 2002; Campbell and Campbell, 2002; Hansen and DeShon, 2002). This approach to mapping depends on scale and density of structures. For example, where the structures are more discrete and separated, we map them separately and not as a specific unit (fig. 3). Where structures are very dense, tend to obscure the underlying terrain, and are embayed by younger material units, we map these pervasive tectonic structures as specific units (fig. 3). We provide detailed images (locations shown in fig. 5) in figures 6–15 to clarify our mapping methods.

Tessera Material

The unit interpreted to be stratigraphically oldest in the map area is tessera material (unit t; figs. 3, 6), which is embayed by most of the other units within the map area. Tessera material is radar bright, is cut by at least two sets of intersecting ridges and grooves, and is a result of tectonic deformation of some precursor terrain (Barsukov and others, 1986; Basilevsky and others, 1986; Bindschadler and Head, 1991; Sukhanov, 1992; sometimes referred to as complex ridged terrain, Solomon and others, 1992; Hansen and others, 1997; Ghent and Hansen, 1999). Arches, ridges, grooves, and graben are tectonic features, so structure is an essential component of the tessera terrain and a key aspect of the unit definition. Globally, tessera occupies about 8 percent of the surface of Venus (Ivanov and Head, 1996) and occurs as large blocks and small islands standing above and embayed by adjacent plains. Three major occurrences of tessera are exposed in the map area: (1) eastern edge of Fortuna Tessera (~900 x 900 km, northwestern map area), (2) Meskhent Tessera (~1,300 x 350 km) in Tethus Regio, and (3) Dekla Tessera (~800 x 300–350 km, southwest corner of map area). The total map area covered by tessera material is about 1.1 x 10^6 km^2 or about 14.1 percent (table 3).

Densely Lineated Plains Material

Among the stratigraphically oldest plains units, densely lineated plains material (unit pdl; figs. 6, 7) is characterized by relatively flat surfaces on a regional scale and by swarms of parallel and subparallel lineaments (resolved as fractures if they are wide enough) having typical spacing of less than 1 km. Occurrences of the unit are typically small, as much as 200–300 km long and 100 km wide, and the total area of the plains is about 0.19 x 10^6 km^2 or approximately 2.4 percent of the area of the quadrangle (table 3). Although the unmodified precursor terrain for the densely lineated plains material is not observed, the flatness of the surface suggests that it was plains. The fractures that deform the surface of the unit are structural elements. They, however, are such a pervasive part of the morphology of this terrain that it becomes a key aspect of the definition of the unit (for example, Campbell and Campbell, 2002; Hansen and DeShon, 2002; Scott and Tanaka, 1986). Densely lineated plains material occurs predominantly around Meskhent Tessera and near the east edge of Fortuna Tessera. The plains are also associated with Dekla Tessera material and nearby belts of ridges.

Ridged Plains Material

Ridged plains material (unit pr; figs. 7, 8) was deformed by relatively broad (5–10 km wide) ridges after its emplacement. In the Meskhent Tessera quadrangle ridged plains material is visible in linear outcrops or belts, in Allat Dorsa, and in unnamed belt fragments, 50–100 km wide and 400–450 km long, and is largely equivalent to the materials forming the ridge belts of Kryuchkov (1990), Frank and Head (1990), Squyres and others (1992) and to units mapped in the other quadrangles on Venus (Rosenberg and McGill, 2001; Ivanov and Head, 2001a; Bridges and McGill, 2002).

Although the ridges that dominate the belts are structural elements, they are important features that help to define and map the material unit of ridged plains. For instance, there is not much doubt that wrinkle ridges deform materials of regional plains. Hypothetically, a wrinkle ridge or a collection of wrinkle ridges would represent kipukas of the regional plains material unit, if younger lavas would flood the rest of the unit. If this hypothetical situation is mapped at a scale sufficient to outline individual exposures (wrinkle ridges) of a material largely covered by younger plains material, then the material deformed by the wrinkle ridges should be mapped as a separate material unit. The scale of our mapping is mostly sufficient to map exposures of a material unit represented on the surface by arches and ridge belts. This is true for unit pr and it is a material unit, although it is represented mostly by structures.

The area occupied by the ridged plains material is about 0.35 10^6 km^2 or approximately 4.6 percent of the quadrangle (table 3). Ridged plains are interpreted to be volcanic plains materials deformed into ridgelike belts by compression. Ridged plains occur primarily in the southwest corner of the map area, where they are in contact with and follow the trend of the Dekla Tessera arc, and in the northeastern map area around Tusholi Corona, where the belts form its east and south rim. In the central map area, ridge belts are associated with Fakahotu Corona and a coronalike feature, Vacuna Corona.

Shield Plains Material

Emplacement of shield plains material (unit psh; figs. 9, 10) of intermediate radar backscatter followed emplacement and deformation of ridged plains material. Shield plains material is characterized by abundant, small, shield-shaped features ranging from a few kilometers in diameter to as much as about 10–20 km; some shields have summit pits. Although small clusters of shields were recognized earlier planetwide (Head and others, 1992), they were thought to be localized occurrences possibly related to individual sources such as hot spots. Later work in Vellamo Planitia (Aubele, 1994, 1995) recognized that many of these occurrences represented a stratigraphic unit in this region, and, subsequently, this unit has been recognized in many areas on the planet (Basilevsky and Head, 1995b; Basilevsky and others, 1997; Crumpler and Aubele, 2000; Addington, 2001; Ivanov and Head, 1998, 2001a,b, 2004), including Meskhent Tessera quadrangle. Shields characterizing this unit occur in clusters, giving the unit a locally hilly texture, and as isolated outcrops in relatively smooth plains. The shields are interpreted to be of volcanic origin and are likely to be the sources of the adjacent smooth plains. In the Meskhent Tessera quadrangle, there is no evidence for specific flows associated with the small edifices of shield plains.

Shield plains material is the most abundant unit in the quadrangle; its area is about 2.14 x 10^6 km^2 or about 28 percent of the map area (table 3). The unit is widely distributed in the map area, and its large fields occur on regional slopes away from the elevated major tessera regions. Numerous outcrops of shield plains also populate the lower surface of Tilli-Hanum Planitia in the southern map area. There are almost no concentrations of shield plains material within the major tesserae and in a vast extension of regional plains in the northeast corner of the map area. Some isolated occurrences of shields are often associated with groove belts of Manto Fossae.

In places, clusters of shields occur where subsequent plains units embay shield plains and form kipukas (flooding the bases of the shields and leaving the tops exposed, fig. 10). Estimates of the thickness (~100–200 m) of the margins of the embaying unit can be made, because the radar brightness of the two units commonly is different and information exists on the topography of the shields (Guest and others, 1992; Kreslavsky and Head, 1999).

Regional Plains Material

After formation of the earlier plains materials, one of the most widespread plains units, regional plains material (units rp_1, rp_2; figs. 7, 9–12), was emplaced. The total area of the plains is about 2.08 x 10^6 km^2 or ~27.1 percent of the quadrangle (table 3). This unit is composed of morphologically smooth, homogeneous plains material of intermediate-dark to interme-

diate-bright radar backscatter complicated by narrow, linear to anastomosing wrinkle ridges (a structural element) in subparallel to parallel lines or intersecting networks. This unit is morphologically similar to the ridged unit of the plateau sequence on Mars (Scott and Tanaka, 1986), which is a plains unit defined by "long, linear to sinuous mare-type (wrinkle) ridges." In the map area, the wrinkle ridges typically are less than 1 km wide and tens of kilometers long; in some areas they may be smaller, whereas in others they are larger. Although their trend often varies locally even within one site, the general orientation of the ridges is predominantly west to east (fig. 4). The unit is interpreted to be regional plains of volcanic origin that were subsequently deformed by wrinkle ridges. Volcanic edifices and sources of the plains are commonly not obvious.

Regional plains material is subdivided into two units by the typical pattern of the radar backscatter. The lower unit (unit rp_1; figs. 7, 9, 10) generally has a homogeneous and relatively low radar backscatter but can be mottled locally. This unit makes up the floor of the lowlands surrounding the major tessera-bearing uplands and occurs predominantly between elongated highs composed of pre-existing units and ridge and groove belts in the western, central, northeastern, and southeastern map area (for example, on the floor of Audra Planitia between individual branches of the Manto Fossae groove zone). The total area of the lower regional plains material is about 1.83×10^6 km^2 or about 23.8 percent of the map area. The upper unit (unit rp_2, fig. 11) appears to have slightly higher radar backscatter and, in places, is characterized by lobate boundaries. The largest areas of this unit occur in the southern and southeastern map area on the floor of Lowana and Tilli-Hanum Planitiae. This unit forms about 0.26×10^6 km^2 or 3.3 percent of the area of the quadrangle.

Plains materials that are younger than regional plains material are characterized either by a morphologically smooth and homogeneous surface or by distinctive lobate and digitate shapes and margins and morphologically smooth surfaces. The surface of these units is commonly unmodified by wrinkle ridges and other structural elements. Two types of the younger plains units are recognized.

Smooth Plains Material

Smooth plains material (unit ps; figs. 12, 13) is characterized by uniform and preferentially low radar backscatter. In places, the radar backscatter of the surface appears to be high (fig. 13). Patches of this unit occur mostly in the north-central map area, where some of them are in close spatial association with coronae Ops and Tusholi and impact craters La Fayette and Jadwiga. The total area of smooth plains is about 0.14×10^6 km^2 or 1.8 percent of the map area (table 3).

Lobate Plains Material

A small area (~0.16×10^6 km^2 or 2.1%) in the eastern portion of the quadrangle is made up of lobate plains material (unit pl; figs. 4, 12, 14) that has internal elements arranged in parallel to sinuous to lobate radar-bright and radar-dark strips and patches; unit boundaries are typically lobate. Individual flowlike features are typically seen on the surface of the plains. Lobate plains material predominantly occurs along a zone of groove belts between Fakahotu Corona and Melia Mons, which appear to be the sources of the plains. Another occurrence of lobate plains surrounds the volcanic center of Amra Tholus in the southern map area.

Shield Cluster Material

The surface of shield cluster material (unit sc; fig. 14) appears to be morphologically similar to that of shield plains (unit psh; figs. 13, 15) but, in contrast, is tectonically undeformed. Small lava flows emanating from the shields are seen in a few places. A small (100–150 km across) field of this unit occurs in association with groove belts (unit gb) and young lava flows (unit pl) on the west flank of Ops Corona. Even smaller occurrences of shield cluster material (tens of kilometers across) are near the summit of Melia Mons, also in association with young lava plains and groove belts. Generally, occurrences of this unit occupy only about 0.008×10^6 km^2 or ~0.1 percent of the map area (table 3).

Impact Crater Material

Impact craters and related deposits are observed in several places in the quadrangle (fig. 4). Their locations are noted by symbols and they are mapped as undivided crater material (unit c; figs. 4, 15) of various diameters that have proximal textured deposits, in some cases, surrounded by crater outflow deposits (unit cf). Two impact craters within the mapped area, Jadwiga and La Fayette, are characterized by distinct, surrounding radar-dark to radar-bright material that partly to wholly obscures the underlying terrain. A large area of dark smooth plains occurs near the crater Jadwiga. In the map area, no craters are embayed by plains materials, and one crater (Faina at lat 71.1° N., long 100.7° E.; 10 km in diameter; table 2) is cut by tectonic features.

Structures

Extensional Structures

Long, linear, radar-bright lineaments are seen in the central and east-central map area and south of the Dekla Tessera arc. In places, paired and inward-facing scarps characterize the lineaments that are interpreted to be graben. The graben are as much as 300–350 km long and, in the central and east-central map area, appear to originate at Fakahotu Corona and a novalike feature at lat 69° N., long 88° E. (Krassilnikov and Head, 2003). The graben and fractures produce a radiating pattern north of the corona and north and south of the nova. The majority of these structures cut the surface of shield plains and regional plains material north of Fakahotu, and graben radiating from the nova are collected into swarms of groove belts that are embayed by regional plains material.

In some cases, the extensional structures, such as fractures and graben, are so closely spaced that they tend to obscure underlying terrain. These concentrations are characterized by numerous long and short curvilinear subparallel lineaments that are usually wide enough to be resolved as fractures and graben. These occurrences form linear belts (groove belts, unit gb; figs. 3, 8, 9) a few hundreds of kilometers long and 50–60 km wide that are slightly elevated compared to the surrounding plains. In detailed mapping at the F-Map scale (75 m/px), remnants of pre-existing plains can be seen between the neighboring tectonic features. Orientations of grooves in the belts are generally parallel to the trend of the groove belts as a whole. Groove belts are concentrated in the west-central and southwestern map area, and a distinctive chain of groove belt occurrences extends northeast from Fakahotu Corona (fig. 3). Groove belts (gb) are distinguished from densely lineated plains material (unit pdl) by their belt-like form, a lower density of tectonic features, and the character of the fractures (more distinctly recognizable graben in unit gb). Groove belts appear to be relatively distinctive stratigraphically. The structures of the belts are mostly embayed by shield plains material (psh) and by regional plains material (units rp_1, rp_2; figs. 8–10). Thus, these plains units represent the upper stratigraphic limit for the groove belts. Where groove belts are in contact with ridge belts, fractures and graben of groove belts cut the surface of ridge belts (fig. 8). Thus, ridged plains material (unit pr) that is usually deformed into ridge belts appears to be the lower stratigraphic limit for groove belts.

Contractional Structures

Several types and scales of contractional features are observed within the quadrangle (figs. 3, 4). Wrinkle ridges are seen throughout the quadrangle but are most prominent in the vast plains, such as regional plains and shield plains (figs. 10, 11). These features are mapped in a representative sense in terms of density and trend by individual wrinkle ridge symbols. In the east half of the quadrangle, there is one predominant, east-west orientation of wrinkle ridges. In the western map area, within the regional low of Audra Planitia between Dekla and Fortuna Tesserae, orientation of wrinkle ridges is south-north, orthogonal to the general trend of the tessera regions.

Wrinkle ridges are common structures within broad fields of shield and regional plains materials (units psh, rp_1, rp_2), which apparently form the stratigraphic base for wrinkle ridge formation. In contrast, there are no wrinkle ridges on the surface of younger plains, such as smooth and lobate plains materials (units ps, pl); these units appear to form an upper stratigraphic limit for wrinkle ridge development within the map area.

Ridges and arches (figs. 3, 7, 8) dominate ridged plains material (unit pr), and their general trends are shown by the map symbols. Ridged plains material forms bands or belts (fig. 3) that are largely equivalent to the ridge belts of Squyres and others (1992). Basilevsky and Head (1995a,b) describe a structure (ridge belt) that is a belt consisting of a cluster of densely spaced ridges 5–10 km wide and a few tens of kilometers long; this unit is often transitional to ridged plains material (unit pr).

Stratigraphic Relations of Units

The mapped material units and structures commonly reveal relations of superposition (embayment) and crosscutting that either clearly display or strongly suggest relative ages among the units. Relations between the oldest units in the map area, tessera material and densely lineated plains material, are shown in figure 6. Densely lineated plains material (unit pdl) occurs as elongated patches, whose surfaces are dissected by densely packed short and narrow lineaments oriented west-northwest. Tessera material (unit t) forms the larger occurrences that are heavily deformed by numerous chaotically organized tectonic structures. These structures are truncated (embayed) at the contact with the densely lineated plains material. More uniformly oriented tectonic structures of unit pdl cut, hence postdate, both tessera and densely lineated plains materials.

Relations between the next oldest units in the map area, densely lineated plains and ridged plains materials, are shown in figure 7. Ridged plains material (unit pr) forms elongated topographic ridges (arches), oriented in northeast and east directions, that are deformed by narrower ridges that are roughly parallel to the arch trends. Dense sets of lineaments oriented preferentially in north and northwest directions cut the surface of an irregularly shaped occurrence of densely lineated plains material (unit pdl). Occurrences of densely lineated plains and ridged plains materials are in direct contact and are characterized by a very dissimilar structural pattern. Pervasive lineaments deforming the surface of unit pdl are completely absent within occurrences of unit pr, whose surface is much less deformed. These differences in the character, density, and orientation of structures suggest that material of ridged plains was emplaced after both emplacement and deformation of material of densely lineated plains. In other localities, however, the relations between these two units are less clear, and densely lineated plains and ridged plains significantly overlap as shown in the Correlation of Map Units.

Clearer relations that are consistent throughout the map area are observed between ridged plains material (unit pr) and groove belts (unit gb; fig. 8). In the area shown in figure 8, two material units (tessera material, unit t, and ridged plains material, unit pr) and one tectonic unit (groove belts, unit gb) are in contact. Tessera material is heavily deformed by at least two sets of tectonic structures that are abruptly terminated by the contact with ridged plains material. The material of ridged plains is ridged to different degrees to form a belt of relatively narrow ridges. The ridges are approximately parallel to each other and oriented north and northwest. The character of the contact between units t and pr is evidence for the older emplacement and deformation of tessera material. Groove belts form a multibranching system of northeast-oriented graben and fracture swarms. Tectonic structures of groove belts clearly cut the surface of both tessera and ridged plains materials and, in turn, are embayed by shield plains material (unit psh).

Clear and consistent relations within the Meskhent Tessera quadrangle exist between groove belts and shield plains material (unit psh). Figure 9*B* shows fragments of a broad zone of densely spaced grooves (a groove belt) that are parallel to each other and oriented northeast. Material that surrounds

occurrences of the groove belt is only slightly deformed and is characterized by abundant small shield features (unit psh). Almost all tectonic structures characterizing the surface of the groove belt terminate at the contact with the shield plains material, which strongly suggests that emplacement of unit psh took place after the main phase of deformation within the groove belt.

Throughout the map area, consistent relations of embayment occur between shield plains material (unit psh) and the lower member of regional plains material (unit rp_1; fig. 10). In many areas within the quadrangle, the shield plains material occurs as tight clusters of small shieldlike structures, which is a characteristic feature of this unit elsewhere on Venus (Crumpler and Aubele, 2000; Addington, 2001; Ivanov and Head, 1997, 2004). Figure 10*B* shows clusters of shields that form a contiguous area with outliers of groove belts surrounded by regional plains material (unit rp_1). The area of shield plains material has a clearly different radar backscatter and typically is outlined by clear sinuous contacts that follow the edges of individual shields at the boundaries of the area (see also Aubele, 1994). There is no evidence for flows emanating from any of the shields and superposed on the surface of surrounding regional plains. The density of shields is sharply diminished across the cluster boundaries, and only several small isolated edifices are seen within neighboring regional plains material. These shields are smaller than those within unit psh and also have no flows superposed on the surrounding plains.

These relations between shield plains and regional plains materials strongly suggest that the shields (clustered or individual) represent kipukas of a unit of shield plains material heavily flooded by younger regional plains material (unit rp_1). Kreslavsky and Head (1999) have shown detailed quantitative examples of such relations that illustrate how isolated shields become smaller and less dense away from the contact, suggesting embayment by younger plains. Although these relative ages are typical within the map area, one cannot rule out the possibility of partly contemporaneous emplacement of shield plains and regional plains. To account for this uncertainty, these two units are shown partly overlapping in the Correlation of Map Units.

Both units of the regional plains material (lower member, unit rp_1; upper member, unit rp_2) are deformed by a pervasive network of wrinkle ridges and, thus, predate the episode(s) of formation of the ridges (figs. 9–11). The upper member of regional plains material is typically brighter in SAR images and, in places, this unit is characterized by lobate boundaries resembling lava flows (fig. 11). These occurrences of the upper member of regional plains material apparently extend along local depressions and tend to outline local highs on the surface of unit rp_1. This suggests that unit rp_2 generally postdates, but may be locally correlative with, the lower member of regional plains material (unit rp_1).

Consistent relations between regional plains material and younger plains units (lobate plains material, unit pl, and smooth plains material, unit ps) are observed within the map area (figs. 12, 13). In each locality where these units are in contact, the lobate and (or) smooth plains materials are nearly undeformed and they embay structures of wrinkle ridges. This means that volcanic activity responsible for the formation of lobate plains began here after formation of wrinkle ridges.

A typical example of an impact crater with outflow deposit (Fedorets, lat 59.7° N., lat 65.6° E., 57.6 km in diameter) is shown in figure 15. The crater is superposed on the lower unit of regional plains material (unit rp_1) and on ridged plains material (unit pr) and postdates episodes of emplacement and deformation of these two units. Because it is stratigraphically younger, the lower unit of regional plains material provides a local lower stratigraphic limit for the impact that produced crater Fedorets. The lower stratigraphic boundaries for impact craters in the Meskhent Tessera quadrangle are listed in table 2; none of the impact craters within the map area appear to have a distinguishable upper stratigraphic limit.

Geologic History

The area of Meskhent Tessera quadrangle is within the topographic province of the midlands (Masursky and others, 1980; Pettengill and others, 1980; Ivanov and Head, 2004c) and illustrates a transitional zone from a large upland of Ishtar Terra to surrounding lowlands, for example Atalanta Planitia (fig. 2a). The map area provides an excellent region for analysis of processes of lowlands and uplands formation and volcanic flooding. Major questions are addressed by geological mapping within the quadrangle: What is the sequence of events in the formation and evolution of large-scale lowlands and uplands on Venus? What are the characteristics of the marginal areas of midlands surrounding these topographic provinces? How did the transition zone of midlands, from the uplands of Ishtar Terra and Tethus Regio to the lowland of Atalanta Planitia, evolve? What information do the units in the Meskhent Tessera quadrangle provide concerning models for Venus global stratigraphy and tectonic history?

The Meskhent Tessera quadrangle (V–3) lies at the east edge of Ishtar Terra, one of the most extensive occurrences of tessera terrain in the northern hemisphere of Venus (Barsukov and others, 1986; Sukhanov, 1992; Ivanov and Head, 1996). In this regional context, the quadrangle represents a sample of terrain where tessera plays an important role. As in many other regions on Venus (Ivanov and Basilevsky, 1993; Ivanov and Head, 1996; Hansen and others, 1997; Phillips and Hansen, 1998), tessera material in the map area is consistently embayed by younger plains material of apparent volcanic origin and, thus, is the stratigraphically oldest unit.

In the map area, tessera material occupies about 1.1×10^6 km^2 (~14.1%, table 3) and forms relatively high standing (figs. 2, 3), complexly deformed areas, the largest of which is exposed in Fortuna Tessera (fig. 1). Smaller massifs of tessera material within the map area are represented by Meskhent Tessera at the east margin of the quadrangle and a tessera arc of Dekla Tessera in the southwestern quadrangle (fig. 1). The principal massif of Fortuna Tessera shows chaotically organized narrow and broad ridges 5–15 km wide that are cut by numerous orthogonal narrow and shallow graben. The same basic set of structures occurs within Meskhent and Dekla Tesserae where, however, the structural pattern is less chaotic and consists mostly of

orthogonal sets of ridges and fractures or graben. Consistent with observations made on regional (Bindschadler and others, 1992a) and global (Ivanov and Head, 1996) scales, tessera material formed from some precursor material that was initially deformed by shortening, folding, and probably shear, which produced more highly deformed terrain than seen in any subsequent units on Venus and then underwent extensional deformation (cut by fractures and graben of various types) to produce the generally orthogonal to chaotic structural fabric typical of much of the tessera planetwide. Other smaller outcrops are exposed as kipukas in the quadrangle; many of them occur near the principal tessera massifs. Based on this distribution and the global distribution of similar small outliers, tessera terrain is thought to exist extensively in the subsurface beneath younger plains units (for example, Ivanov and Head, 1996). Whether this distribution is planetwide, regional, or even local is unclear. No direct evidence exists in the map area for the duration of tessera formation, but global crater studies (Ivanov and Basilevsky, 1993; Gilmore and others, 1996) suggest a relatively short duration (for example, tens of millions of years).

Sometimes marginal to the tessera terrain and embaying it, the plains material has been densely fractured (unit pdl) and, in some cases, has a structural fabric orientation similar to the latest phase of deformation in tessera (fig. 6). The deformation patterns in densely lineated plains material are very dense (spacing <1 km and as low as the resolution limit of the Magellan images, ~75 m/pixel) and unidirectional, and the role of extension in the formation of the structural pattern of unit pdl is evident. Along the north margin of Meskhent Tessera, an east-west-oriented band of densely lineated plains material is characterized by a very dense set of northwest-oriented structures. Features of the plains appear to continue the structural trend of some of the set of structures in the tessera material, but the deformation patterns in densely lineated plains material are unidirectional in contrast to the orthogonal patterns of tessera (fig. 6). The morphology and planimetric shape of the structures of densely lineated plains material suggest that both tensile and shear stresses have been involved in the deformation. Although occurrences of the plains material are heavily deformed by secondary structures, the overall flatness of the surface suggests that the precursor material had a volcanic origin. This unit is interpreted to be volcanic plains material that embayed early tessera but that was deformed by the latest phases of tessera deformation. Densely lineated plains are, thus, partly laterally equivalent to tessera, and the north margin of Meskhent Tessera is an example of such a transition.

Densely lineated plains material makes up a small percentage of the surface outcrop (~2.4%, table 3) and occurs as locally elevated, small (tens of kilometers across) areas throughout the quadrangle. Such a distribution suggests a more extensive presence of the unit in the subsurface, regardless of the present regional topographic configuration of territory within the quadrangle.

A less deformed plains unit (ridged plains material, unit pr) was emplaced either contemporaneously or, in part, following the formation of densely lineated plains material (fig. 7). Although little evidence exists for sources, the smooth surface texture of the background material of the unit strongly suggests that it had a volcanic origin. The most important features of ridged plains are ridges, usually curvilinear structures 5–10 km wide, that are pervasive. The ridges are comparable to contractional structures of the lunar mare. Occurrences of the unit make up about 4.6 percent of the surface of the quadrangle and typically form zones of broad arches (as much as 50–100 km across). One of these zones runs generally parallel to the strike of the arc of tessera material of Dekla Tessera (fig. 3). In the northeastern map area, elongated occurrences of the ridged plains material deformed by the ridges form the eastern and southern parts of the rim of Tusholi Corona. Ridged plains material is also associated with coronae in the central map area, where it forms the southern rim of Fakahotu Corona and outlines a coronalike feature, Vacuna Corona, on the south and east.

The parallelism of the trend of the tectonic structures (ridges) and broad arches of the ridged plains material suggests the same principal strain orientation during formation of both types of features. Thus, the period during which this unit was formed was characterized by emplacement of volcanic plains and their subsequent deformation into broad arches with distinctive ridges. The material of unit pr and its deformation appear to have produced the second-order topography within extensive lowlands in the central and north-central Meskhent Tessera quadrangle.

Within the Meskhent Tessera quadrangle, distinct zones of fractures and graben (groove belts, structural unit gb) are abundant (~11.9% of map area). There are two main occurrences of groove belts in the quadrangle. One (Manto Fossae) forms a giant arclike zone about 2,500 km long that extends from the center of Audra Planitia in a low-lying area between Dekla and Fortuna Tesserae to the east and then to the southeast along the trend of both Dekla Tessera and belts of ridges near Dekla. Another broad (~1,000 km wide) area of groove belts occurs in the southwest corner of the quadrangle. Subparallel branches of groove belts from this zone are oriented northeast, almost perpendicular to the strike of the Manto Fossae groove belts. Formation of the belts of graben marks the episodes of extension that were both parallel and radial to the orientation of the Dekla tessera arc. The relative time of formation between the major systems of groove belts within the map area cannot be established, however, due to lack of unambiguous crosscutting relations among the systems.

The time of the formation of groove belts as a whole, however, appears to be well constrained in the map area. Structural elements (fractures and graben) of groove belts cut the surface of ridged plains material (unit pr; fig. 8) where groove belts and unit pr are in contact. Thus, groove belts appear to begin after emplacement and deformation of ridged plains material. Materials of the younger plains (shield plains material and regional plains material; figs. 8–10) embay most of the structures of groove belts, implying that the main episode of development of groove belts preceded formation of the vast plains materials.

Prominent deformational zones of ridge belts and groove belts (Barsukov and others, 1986; Sukhanov and others, 1989) characterize the map area (fig. 3). Small arcuate segments of ridge belts form parts of the rim of Tusholi, Vacuna, and Fakahotu Coronae. These belts most likely represent local zones of

contractional deformation related to specific stages of evolution of coronae that predated emplacement of the material of the vast plains units, such as shield plains and regional plains (units psh and rp_1). Ridge belts occur preferentially in the west half of the quadrangle along the north side of the large arclike Dekla tessera. This type of association of ridge belts is not common on Venus (Ivanov and Head, 1996) and probably requires a mechanism of formation that is different from that proposed for the belts within the giant fan-shaped zone centered at about long 220° E. (Zuber, 1987; Frank and Head, 1990; Kruychkov, 1990; Sukhanov and Pronin, 1989; Young and Hansen, 2005). Close spatial association of ridge belts with Dekla Tessera and their preferential occurrence along only one (north) side of the tessera arc (fig. 3) may imply that these belts were formed by lateral compression in the north-south direction and deformation of suites of lava plains against a rigid foreland formed by the tessera massif. Stratigraphic relations between tessera, ridge belts, and vast plains units suggest that the main phase of ridge belt formation near Dekla postdated tessera and that the deformation largely waned before emplacement of material of shield plains.

Major zones of groove belts occur throughout the Meskhent Tessera quadrangle (fig. 3). In the west half of the map area, groove belts occur as a large arc forming Manto Fossae, which is broadly parallel to the elongation of Dekla Tessera. In the southwest corner of the map area, another extensive zone of groove belts mostly confined within the Dekla Tessera arc is oriented almost orthogonal to the strike of the Manto Fossae zone. Neither coronae nor large volcanic centers are associated with these zones, and there is little evidence for younger volcanic activity along the belts.

A segment of a groove belt in the eastern map area between Fakahotu Corona and the large volcano of Melia Mons is significantly different. This belt is the southwestern extension of a prominent zone of groove belts and coronae that characterizes the west margin of the lowland of Atalanta Planitia (Ivanov and Head, 2004a). The complex of coronae and groove belts within the Meskhent (V–3) and Atalanta Planitia (V–4) quadrangles strongly resemble the groove belt/corona zones that outline the east and south margins of Lavinia Planitia (Baer and others, 1994; Magee and Head, 1995; Ivanov and Head, 2001a) and the rift/corona zones typical of eastern Aphrodite Terra (Bleamaster and Hansen, 2004).

The relations of the belts with coronae and younger volcanic activity suggest that the groove belts inside and outside the Dekla Tessera arc, and the belt between Fakahotu Corona and Melia Mons, may represent two different classes of extensional zones. The belts in the western quadrangle (V–3) may have formed due to tectonic response of the lithosphere to possible gravitational readjustment of the large massifs of Dekla and Tellus Tesserae (passive rifting). In contrast, the belt in the eastern quadrangle (V–4) most likely is the result of mutual development of lithospheric extension (active rifting) and diapirism. The stratigraphic relations suggest that the distinctive pulse of volcanism in the evolution of the groove belt/corona complex, marked by the emplacement of the lobate plains, occurred significantly later than the main phase of tectonic deformation, which predates the material of regional plains.

After emplacement and deformation of ridged plains and formation of groove belts, another distinctly different plains unit (shield plains material, unit psh) was emplaced in many parts of the map area. Shield plains material is the most abundant unit within the quadrangle, forming about 2.43×10^6 km^2 or approximately 31.7 percent of the map area. The unit is exposed throughout the Meskhent Tessera quadrangle but is noticeably absent in its northwest and northeast corners occupied by Fortuna Tessera and a large extension of regional plains. The abundant shield volcanoes and intershield plains material that are characteristic of this unit differ from the volcanic style of emplacement of both previous ridged plains material and subsequent regional plains material. The abundance of shield volcanoes indicates widespread local and shallow magma sources during the emplacement of shield plains material. Material unit psh embays ridged plains material and most structures of the groove belts (figs. 8, 9) and, thus, it is a younger unit. The shieldlike edifices of unit psh are typically embayed by material of regional plains (fig. 9, 10). This strongly suggests that shield plains material predates emplacement of units of regional plains materials.

Close association of the shield plains with older units such as tessera and ridged plains materials and elevated branches of groove belts that make up local highs suggests that the topographic position of the unit was an important factor in their present areal distribution (Ivanov and Head, 2001b, 2004). This is consistent with broad embayment of the shield plains unit by later plains (Kreslavsky and Head, 1999) and, based on the outcrop patterns of subsequent units, shield plains material probably underlies a significant portion of the younger plains material within the quadrangle. The lack of extensive development of contractional features, such as arches and ridge belts, within the areas of unit psh could imply that regional compressional stresses had further waned before emplacement of the unit.

Subsequent to the emplacement of shield plains material, the style of volcanism changed again (Head and others, 1996). Instead of abundant small shield volcanoes, broad units of regional plains material were emplaced from sources that are now rarely visible. The wide extent of these units, especially of the lower member (unit rp_1) within the quadrangle and elsewhere and the presence on its surface of narrow sinuous channels (Baker and others, 1992, 1997; Komatsu and Baker, 1994; Basilevsky and Head, 1996), suggests a high-effusion-rate mode of emplacement from a few sources. Such a volcanic style during the formation of regional plains material is in distinct contrast to the widespread and abundant small shield volcanoes just preceding this phase. Although widespread, regional plains material appears to be relatively thin (Ivanov and Head, 2001b; de Shon and others, 2000), because small and large outliers of older units commonly occur within the broad fields of regional plains.

On the basis of the outcrop distribution of the upper member of regional plains material (unit rp_2), the sources of this unit may have been distributed mostly in the southern and southeastern map area; two centers, Malintzin Patera and Amra Tholus (fig. 1), appear to be the sources of unit rp_2. These sources may have fed individual deposits in smaller secondary

basins that complicate the broad low-lying plains of Lowana Planitia. The largest occurrence of the unit rp_2 is in the southeast corner of the map area, and its source region appears to be outside of the Meskhent Tessera quadrangle. Materials of regional plains (units rp_1, rp_2) cover about 30.9 percent of the map area (table 3) and make up the floor of broad plains between the major areas of tessera.

The volcanic plains of units rp_1 and rp_2, as well as previous shield plains material (unit psh), were further deformed by structures of wrinkle ridges apparently subsequent to their emplacement. The orientation of wrinkle ridges on the surface of these units generally does not correlate with the older structural trends of ridged plains material (unit pr) and the tectonic unit of groove belts (unit gb). Thus, the deformation recorded in material units, rp_1 and rp_2, appears to be poorly related to older structural trends and also reflects a decreasing amount of shortening and deformation with time.

Occurrences of smooth plains material (unit ps) with homogeneous radar backscatter, which is usually low, were emplaced mostly in the north-central map area in a broad topographic trough separating Fortuna Tessera from Tethus Regio. Smooth plains material is in spatial association with Ops and Tusholi Coronae, which are the likely sources for unit ps. In this area, however, some of the occurrences of smooth plains material also appear to be a continuation of a parabola-like feature (deposit) related to impact craters La Fayette and Jadwiga (fig. 4). These occurrences of smooth plains material suggest that, to some degree, this material may be related to the deposition and redistribution of debris material that was formed after the impact events (fig. 13).

After formation of regional plains material, relatively small occurrences of lobate and digitate flows were emplaced (fig. 12). Contiguous occurrences of these flows make up lobate plains material (unit pl), which covers a small area (~0.16 x 10^6 km^2 or 2.1%) within the quadrangle and is closely associated with three distinct source areas: Fakahotu Corona, Melia Mons, and Amra Tholus. Fakahotu Corona and Melia Mons are connected by a distinct zone of groove belts. The belts are the southwestern extension of a larger zone of coronae interconnected by swarms of grooves that characterize the west margin of the Atalanta Planitia basin within the Meskhent Tessera quadrangle (Ivanov and Head, 2004). There is no evidence for the deformation of these flows by wrinkle ridges, which suggests that the flows are either very recent and undeformed or that wrinkle ridge deformation as a general phenomena ceased by this time. On the basis of the general decrease in intensity of tectonic deformation as a function of time, we interpret the general absence of wrinkle ridges in lobate plains to be the result of waning deformational forces.

Evidence from Fakahotu and Ops Coronae and the corona-like Melia Mons suggests that these features were active for a long period of time. Early episodes of formation of these volcano-tectonic complexes are manifested by structural elements such as groove swarms and belts of ridges that predate emplacement of regional plains. Final phases of activity are related to formation of young volcanic plains and flows (lobate plains) that are superposed on regional plains. Volcanism at the time of the emplacement of lobate plains material was much less abundant than during episodes of formation of shield plains, regional plains material, and extensive digitate and lobate flows associated with coronae and intermediate/large volcanoes.

Of the twelve impact craters seen in the map area (figs. 1, 4; table 2), we observed only one example of an impact crater (Faina, lat 71.1° N., long 99.9° E.; 4.5 km diameter) that is deformed by tectonic structures. The crater is in a zone of groove belts that makes up the north rim of Tusholi Corona. Structures of the belt cut the crater and, therefore, the crater was formed during the active phase of groove belt evolution. There are no craters in the map area that are embayed by volcanic activity. Thus, impact craters appear to be younger than the material units on which they are superposed. Eight craters out of twelve (~66%) postdate the lower unit of regional plains material (unit rp_1). Two craters (~17%) are younger than shield plains material. Two more craters (~17%) are superposed on groove belts; one of these craters (Faina) appears to have formed contemporaneously with the belt.

In summary, there are clear trends in the evolution of both tectonic regimes and style of volcanism within the Meskhent Tessera quadrangle. Contractional deformation changed from deformation associated with the formation of compact ridge belts (unit pr; figs. 6, 7) to deformation of regional plains (material units rp_1 and rp_2) by pervasive structures of wrinkle ridges (figs. 8, 9). Contractional structures are absent within younger plains units, such as smooth and lobate plains materials (units ps, pl; figs. 11, 12), suggesting cessation of compression stresses by the time of emplacement of these units.

Extensional deformation that overprints densely lineated plains material (unit pdl) and played a major role in the formation of groove belts (gb) appears to be more prominent as a function of time. Fractures that have shaped the surface of material unit pdl are very narrow, pervasive, and do not form beltlike concentrations. The subsequent occurrences of extensional structures are organized into belts whose individual structures, on average, become progressively broader as a function of time.

The changes in character of broad-scale volcanic activity are clearly recorded in units beginning with shield plains material. Formation of this unit is related to numerous small individual volcanic constructs. This mode of volcanism changed to massive volcanic flooding from unrecognizable sources during emplacement of the lower unit of regional plains material (unit rp_1). Later plains units, such as the upper unit of regional plains material (unit rp_2), smooth plains material (unit ps), and lobate plains material (unit pl), were related to large distinct sources, such as some coronae and intermediate and large volcanoes. Coronae within the map area display prolonged evolution. They started to form apparently early during formation of heavily tectonized units, such as ridged plains material and groove belts. Evolution of coronae continued through the majority of the geological record and apparently ended with the emplacement of young smooth and lobate plains materials and small clusters of shields.

The presence of the trends in endogenous activity documented within the Meskhent Tessera quadrangle is consistent with the evolutionary model of geologic history of Venus (for example, Basilevsky and Head, 1998; Ivanov and Head, 2001b). These trends, however, contradict the predictions of the non-

directional (patchwork) model of Venus history (Guest and Stofan, 1999).

Acknowledgements

Thanks are extended to Alexander Basilevsky and Jayne Aubele for detailed discussion about regional and global units and relations. We particularly appreciate the helpful discussions that occurred during the annual National Aeronautics and Space Administration (NASA) mappers meetings and during an informal mapping workshop held at Brown University in the summer of 1995 and attended by George McGill, Steve Saunders, Jim Zimbelman, Alexander Basilevsky, Elizabeth Rosenberg, and Nathan Bridges. Their comments and discussions were most helpful. Reviews of the map materials by Robert Brackenridge and George McGill are deeply appreciated. Financial support from the NASA Planetary Geology and Geophysics Program (Grant NAGW-5023) is gratefully acknowledged.

References Cited

Addington, E.A., 2001, A stratigraphic study of small volcano clusters on Venus: Icarus, v. 149, p. 16–36.

American Commission on Stratigraphic Nomenclature, 1961, Code of Stratigraphic Nomenclature: American Association of Petroleum Geologists Bulletin, v. 45, no. 5 p. 645–665.

Aubele, J.C., 1994, Stratigraphy of small volcanoes and plains terrain in Vellamo Planitia, Venus [abs.], *in* Lunar and Planetary Science Conference, 25th, March 14–18, 1994: Houston, Tex., Lunar and Planetary Institute, p. 45–46.

Aubele, J.C., 1995, Stratigraphy of small volcanoes and plains terrain in Vellamo Planitia-Shimti Tessera region, Venus [abs.], *in* Lunar and Planetary Science Conference, 26th, March 13–17, 1995: Houston, Tex., Lunar and Planetary Institute, p. 59–60.

Aubele, J.C., and Slyuta, E.N., 1990, Small domes on Venus—Characteristics and origin: Earth, Moon, and Planets, v. 50/51, p. 493–532.

Baer, G., Schubert, G., Bindschadler, D.L., and Stofan, E.R., 1994, Spatial and temporal relations between coronae and extensional belts, northern Lada Terra, Venus: Journal of Geophysical Research, v. 99, p. 8355–8369.

Baker, V.R., Komatsu, G., Gulick, V.C., and Parker, T.J., 1997, Channels and valleys, *in* Phillips, R., and others, eds., Venus II: Tucson, University of Arizona Press, p. 757–793.

Baker, V.R., Komatsu, G., Parker, T.J., Gulick, V.C., Kargel, J.S., and Lewis, J.S., 1992, Channels and valleys on Venus—Preliminary analysis of Magellan data: Journal of Geophysical Research, v. 97, p. 13,421–13,444.

Barsukov, V.L., Basilevsky, A.T., Burba, G.A., and 27 others, 1986, The geology and geomorphology of the Venus surface as revealed by the radar images obtained by Veneras 15 and 16: Journal of Geophysical Research, v. 91, p. D378–D398.

Basilevsky, A.T., and Head, J.W., 1995a, Global stratigraphy of Venus—Analysis of a random sample of thirty-six test areas: Earth, Moon, and Planets, v. 66, p. 285–336.

Basilevsky, A.T., and Head, J.W., 1995b, Regional and global stratigraphy of Venus—A preliminary assessment and implications for the geologic history of Venus: Planetary Space Science, v. 43, p. 1523–1553.

Basilevsky, A.T., and Head, J.W., 1996, Evidence for rapid and widespread emplacement of volcanic plains on Venus—Stratigraphic studies in the Baltis Vallis region: Geophysical Research Letters, v. 23, p. 1497–1500.

Basilevsky, A.T., and Head, J.W., 1998, The geologic history of Venus—A stratigraphic view: Journal of Geophysical Research, v. 103, p. 8531–8544.

Basilevsky, A.T., and Head, J.W., 2000, Geologic units on Venus—Evidence for their global correlation: Planetary Space Science, v. 48, p. 75–111.

Basilevsky, A.T., Head, J.W., Schaber, G.G., and Strom, R.G., 1997, The resurfacing history of Venus, *in* Phillips, R., and others, eds., Venus II: Tucson, University of Arizona Press, p. 1047–1084.

Basilevsky, A.T., Head, J.W., and Setyaeva, I.V., 2003, Venus—Estimation of age of impact craters on the basis of degree of preservation of associated radar-dark deposits: Geophysical Research Letters, v. 30 (doc. no.: 1950, doi: 10.1029/2003GL017504).

Basilevsky, A.T., Nikolaeva, O.V., and Weitz, C.M., 1992, Geology of the Venera 8 landing site region from Magellan data—Morphological and geochemical considerations: Journal of Geophysical Research, v. 97, p. 16,315–16,335.

Basilevsky, A.T., Pronin, A.A., Ronca, L.B., Kryuchkov, V.P., Sukhanov, A.L., and Markov, M.S., 1986, Styles of tectonic deformations on Venus—Analysis of Venera 15 and 16 data *in* Proceedings of the 16th Lunar and Planetary Science Conference, Part 2: Journal of Geophysical Research, v. 91. p. D399–D411.

Bindschadler, D.L., Decharon, A., Beratan, K.K., Smrekar, S.E., and Head, J.W., 1992a, Magellan observations of Alpha Regio—Implications for formation of complex ridged terrains on Venus: Journal of Geophysical Research, v. 97, p. 13,563–13,578.

Bindschadler, D.L., and Head, J.W., 1991, Tessera terrain, Venus—Characterization and models for origin and evolution: Journal of Geophysical Research, v. 96, p. 5889–5907.

Bindschadler, D.L., Schubert, G., and Kaula, W.M., 1992b, Coldspots and hotspots—Global tectonic and mantle dynamics of Venus: Journal of Geophysical Research, v. 97, p. 13,495–13,532.

Bleamaster, L.F., and Hansen, V.L., 2004, Effects of crustal heterogeneity on the morphology of chasmata: Journal of Geophysical Research, v. 109 (doc. no.: E09004, doi: 10.1029/2003JE002913).

Bondarenko, N.V., and Head, J.W., 2004, Radar-dark impact crater-related parabolas on Venus—Characterization of deposits with Magellan emissivity data: Journal of Geophysical Research, v. 109 (doc. no.: E09004, doi: 10.1029/2004JE002256).

Bridges, N.T., and McGill, G.E., 1999, Recent tectonic and lithospheric thermal evolution of Venus: Icarus, v. 139, p. 40–48.

Bridges, N.T., and McGill, G.E., 2002, Geologic map of the Kaiwan Fluctus quadrangle (V–44), Venus: U.S. Geological Survey Geologic Investigations Series Map I–2747 [http://pubs.usgs.gov/imap/i2747/].

Campbell, B.A., 1995, Use and presentation of Magellan quantitative data in Venus mapping: U.S. Geological Survey Open-File Report 95–519, 32 p.

Campbell, B.A., 1999, Surface formation rates and impact crater densities on Venus: Journal of Geophysical Research, v. 104, p. 21,951–21,955.

Campbell, B.A., and Campbell, P.G., 2002, Geologic map of the Bell Regio quadrangle (V–9), Venus: U.S. Geological Survey Geologic Investigations Series Map I–2743 [http://geopubs.wr.usgs.gov/i-map/i2743/].

Campbell, D.B., Stacy, N.J.S., Newman, W.I., and 5 others, 1992, Magellan observations of extended crater related features on the surface of Venus: Journal of Geophysical Research, v. 97, p. 16,249–16,277.

Crumpler, L.S., and Aubele, J.C., 2000, Volcanism on Venus, *in* Encyclopedia of Volcanoes: Academic Press, p. 727–770.

Crumpler, L.S., Head, J.W., and Aubele, J.C., 1993, Relation of major volcanic center concentration on Venus to global tectonic patterns: Science, v. 261, p. 591–595.

DeShon, H.R., Young, D.A., and Hansen V.L., 2000, Geologic evolution of southern Rusalka Planitia: Journal of Geophysical Research, v. 105, p. 6983–6996.

Elachi, C., 1987, Introduction to the physics and techniques of remote sensing: New York, Wiley and Sons, 413 p.

Figueredo, P.H., and Greeley, R., 2000, Geologic mapping of the northern leading hemisphere of Europa from Galileo solid-state imaging data: Journal of Geophysical Research, v. 105, p. 22,629–22,646.

Ford, P.G., and Pettengill, G.H., 1992, Venus topography and kilometer-scale slopes: Journal of Geophysical Research, v. 97, p. 13,102–13,114.

Ford, P.G., Plaut, J.J., Weitz, C.M., and 5 others, 1993, Guide to Magellan image interpretation: Jet Propulsion Laboratory, Publication 93–24, 148 p.

Frank, S.L., and Head, J.W., 1990, Ridge Belts on Venus—Morphology and Origin: Earth, Moon, and Planets, v. 50/51, p. 421–470.

Ghent, R., and Hansen, V., 1999, Structural and kinematic analysis of eastern Ovda Regio, Venus—Implications for crustal plateau formation, Icarus, v. 139, p. 116–136.

Gilmore, M.S., Ivanov, M.A., Head, J.W., and Basilevsky, A.T., 1996, Duration of tessera deformation on Venus: Journal of Geophysical Research, v. 102, p. 13,357–13,368.

Greeley, R., Arvidson, R.E., Elachi, C., and 8 others, 1992, Aeolian features on Venus—Preliminary Magellan results: Journal of Geophysical Research, v. 97, p. 13,319–13,345.

Grimm, R.E., 1994, The deep structure of venusian plateau highlands: Icarus, v. 112, p. 89–103.

Guest, J.E., Bulmer, M.H., Aubele, J., and 6 others, 1992, Small volcanic edifices and volcanism in the plains of Venus: Journal of Geophysical Research, v. 97, p. 15,949–15,966.

Guest, J.E., and Stofan, E.R., 1999, A new view of the stratigraphic history of Venus: Icarus, v. 139, p. 56–66.

Hansen, V.L., 2000, Geologic mapping of tectonic planets: Earth and Planetary Science Letters, v. 176, p. 527–542.

Hansen, V.L., and DeShon, H.R., 2002, Geologic map of the Diana Chasma quadrangle (V–9), Venus: U.S. Geological Survey Geologic Investigations Series Map I–2752 [http://pubs.usgs.gov/imap/i2752/].

Hansen, V.L., Willis, J.J., and Banerdt, W.B., 1997, Tectonic overview and synthesis, *in* Phillips, R., and others, eds., Venus II: Tucson, University of Arizona Press, p. 797–844.

Hauck, S.A., Phillips, R.J., and Price, M.H., 1998, Venus—Crater distribution and plains resurfacing models: Journal of Geophysical Research, v. 103, p. 13,635–13,642.

Head, J.W., Basilevsky, A.T., Wilson, L., and Hess, P.C., 1996, Evolution of volcanic styles on Venus—Change, but not Noachian? [abs.], *in* Lunar and Planetary Science Conference, 27th, March 13–17, 1996: Houston, Tex., Lunar and Planetary Institute, p. 525–526.

Head, J.W., Crumpler, L.S., Aubele, J.C., Guest, J.E., and Saunders, R.S., 1992, Venus volcanism—Classification of volcanic features and structures, associations, and global distribution from Magellan data: Journal of Geophysical Research, v. 97, p. 13,153–13,197.

Herrick, R.R., Sharpton, V.L., Malin, M.C., Lyons, S.N., and Feely, K., 1997, Morphology and morphometry of impact craters, *in* Phillips, R., and others, eds., Venus II: Tucson, University of Arizona Press, p. 1015–1046.

Ivanov, B.A., Nemchinov, I.V., Svetsov, V.A., Provalov, A.A., Khazins, V.M., and Phillips, R.J., 1992, Impact cratering on Venus—Physical and mechanical models: Journal of Geophysical Research, v. 92, p. 16,167–16,181.

Ivanov, M.A., and Basilevsky, A.T., 1993, Density and morphology of impact craters of tessera terrain, Venus: Geophysical Research Letters, v. 20, p. 2579–2582.

Ivanov, M.A., and Head, J.W., 1996, Tessera terrain on Venus—A survey of the global distribution, characteristics, and relation to surrounding units: Journal of Geophysical Research, v. 101, p. 14,861–14,908.

Ivanov, M.A., and Head, J.W., 1997, Areal and stratigraphic distribution of the steep sided domes—Preliminary results of the regional mapping of Venus, *in* Lunar and Planetary Science Conference, 28th, March 16–20, 1998: Houston, Tex., Lunar and Planetary Institute, p. 639–640.

Ivanov, M.A., and Head, J.W., 1998, Major issues in Venus geology—Insights from a global geotraverse at 30N latitude [abs.], *in* Lunar and Planetary Science Conference, 29th, March 16–20, 1998: Houston, Tex., Lunar and Planetary Institute, Abstract #1419.

Ivanov, M.A., and Head, J.W., 1999, The stratigraphic and geographic distribution of steep-sided domes on Venus—Preliminary results from regional geologic mapping and implications for their origin: Journal of Geophysical Research, v. 104, p. 18,907–18,924.

Ivanov, M.A., and Head, J.W., 2001a, Geologic map of the Lavinia Planitia quadrangle (V–55): U.S. Geological Survey Miscellaneous Investigations Series Map I–2684, scale 1:5,000,000 [http://pubs.usgs.gov/imap/i2684/].

Ivanov, M.A., and Head, J.W., 2001b, Geology of Venus—Mapping of a global geotraverse at 30N latitude: Journal of Geophysical Research, v. 106, p. 17,515–17,566.

Ivanov, M.A., and Head, J.W., 2004a, Geologic map of the Atalanta Planitia quadrangle (V–4), Venus: U.S. Geological Survey Geologic Investigations Series Map I–2792 [http://pubs.usgs.gov/imap/i2792/].

Ivanov, M.A., and Head, J.W., 2004b, Stratigraphy of small shield volcanoes on Venus—Criteria for determining stratigraphic relationships and assessment of relative age and temporal abundance: Journal of Geophysical Research, v. 109 (doc. no.: NE10001, doi: 10.1029/2004JE002252).

Ivanov, M.A., and Head, J.W., 2004c, Solar System—Venus, *in* Encyclopedia of Geology: New York, Elsevier, p. 244–264.

Ivanov, M.A., and Head, J.W., 2005, Geologic map of the Mylitta Fluctus quadrangle (V–61), Venus: U.S. Geological Survey Scientific Investigations Map 2920 [http://pubs.usgs.gov/sim/2006/2920/].

Komatsu, G., and Baker, V.R., 1994, Longitudinal profiles of plains channels on Venus, *in* Lunar and Planetary Science Conference, 25th, March 16–20, 1994: Houston, Tex., Lunar and Planetary Institute, p. 727–728.

Konopliv, A.S., Banerdt, W.B., and Sjogren, W.L., 1999, Venus gravity—180th degree and order model: Icarus, v. 139, p. 3–18.

Konopliv, A.S., and Sjogren, W.L., 1994, Venus spherical harmonic gravity model to degree and order 60: Icarus, v. 112, p. 42–54.

Krassilnikov, A.S., and Head, J.W., 2003, Novae on Venus—Geology, classification and evolution: Journal of Geophysical Research, v. 108, (doc. no.: 5108, doi: 10.1029/2002JE001983).

Kreslavsky, M.A., and Head, J.W., 1999, Morphometry of small shield volcanoes on Venus—Implications for the thickness of regional plains: Journal of Geophysical Research, v. 104, p. 18,925–18,932.

Kryuchkov, V.P., 1990, Ridge Belts—Are they compressional or extensional structures?: Earth, Moon, and Planets, v. 50/51, p. 471–491.

Magee, K.P., and Head, J.W., 1995, The role of rifting in the generation of melt—Implications for the origin and evolution of the Lada Terra-Lavinia Planitia region on Venus: Journal of Geophysical Research, v. 100, p. 1527–1552.

Masursky, H., Eliason, E., Ford, P.G., and 4 others, 1980, Pioneer-Venus radar results—Geology from the images and altimetry: Journal of Geophysical Research, v. 85, p. 8232–8260.

McKinnon, W.B., Zahnle, K.J., Ivanov, B.A., and Melosh, H.J., 1997, Cratering on Venus—Models and observations, *in* Phillips, R., and others, eds., Venus II: Tucson, University of Arizona Press, p. 969–1014.

Mescherikov, Y.A., 1968, Plains, *in* Fairbridge, R.W., Encyclopedia of Geomorphology: New York, Reinhold Book Corporation, 1,295 p.

North American Commission on Stratigraphic Nomenclature, 1983, Code of Stratigraphic Nomenclature: American Association of Petroleum Geologists Bulletin, v. 67, p. 841–875.

Pavri, B., Head, J.W., Klose, K.B., and Wilson, L., 1992, Steep-sided domes on Venus—Characteristics, geologic setting, and eruption conditions from Magellan data: Journal of Geophysical Research, v. 97, p. 13,445–13,478.

Pettengill, G.H., Eliason, E., Ford, P.G., Loriot, G.B., Masursky, H., and McGill, G.E., 1980, Pioneer Venus radar results—Altimetry and surface properties: Journal of Geophysical Research, v. 85, p. 8261–8270.

Phillips, R.J., and Hansen, V.L., 1998, Geological evolution of Venus—Rises, plains, plumes, and plateaus: Science, v. 279, p. 1492–1497.

Phillips, R.J., Raubertas, R.F., Arvidson, R.E., and 4 others, 1992, Impact craters and Venus resurfacing history: Journal of Geophysical Research, v. 97, p. 15,923–15,948.

Pronin, A.A., and Stofan, E.R., 1990, Coronae on Venus—Morphology and distribution: Icarus, v. 87, p. 452–474.

Raitala, J., 1996, Meshkenet Tessera—Echelon megafaults and surface relaxation on Venus: Bulletin of the American Astronomical Society, v. 28, p. 1118–1119.

Rosenberg, E., and McGill, G.E., 2001, Geologic map of the Pandrosos Dorsa quadrangle (V–5), Venus: U.S. Geological Survey Geologic Investigations Series Map I–2721 [http://pubs.usgs.gov/imap/i2721/].

Saunders, R.S., and 26 others, 1992, Magellan mission summary: Journal of Geophysical Research, v. 97, p. 13,067–13,090.

Schaber, G.G., Kirk, R.L., and Strom, R.G., 1998, Data base of impact craters on Venus based on analysis of Magellan radar images and altimetry data: U.S. Geological Survey Open-File Report 98–104.

Schaber, G.G., Strom, R.G., Moore, H.J., and 7 others, 1992, Geology and distribution of impact craters on Venus—What are they telling us?: Journal of Geophysical Research, v. 97, p. 13,257–13,302.

Schultz, P., 1992, Atmospheric effects on ejecta emplacement and crater formation on Venus from Magellan: Journal of Geophysical Research, v. 97, p. 183–248.

Scott, D.H., and Tanaka, K.L., 1986, Geologic map of the western equatorial region of Mars: U.S. Geological Survey Miscellaneous Investigations Series Map I–1802–A, scale 1:15,000,000.

Solomon, S.C., Smrekar, S.E., Bindschadler, D.L., and 8 others, 1992, Venus tectonics—An overview of Magellan observations: Journal of Geophysical Research, v. 97, p. 13,199–13,256.

Squyres, S.W., Jankowski, D.G., Simons, M., and 3 others, 1992, Plains tectonism on Venus—The deformation belts of Atalanta Planitia: Journal of Geophysical Research, v. 97, p. 13,579–13,600.

Stofan, E.R., Anderson, S.W., Crown, D.A., and Plaut, J.J., 2000, Emplacement and composition of steep-sided domes on Venus: Journal of Geophysical Research, v. 105, p. 26,757–26,771.

Stofan, E.R., and Head, J.W., 1990, Coronae of Mnemosyne Regio—Morphology and origin: Icarus, v. 83, p. 216–243.

Stofan, E.R., Sharpton, V.L., Schubert, G., and 4 others, 1992, Global distribution and characteristics of coronae and related features on Venus—Implications for origin and

relation to mantle processes: Journal of Geophysical Research, v. 97, p. 13,347–13,378.
Stofan, E.R., Smrekar, S.E., Tapper, S.W., Guest, J.E., and Grindrod, P.M., 2001, Preliminary analysis of an expanded corona database for Venus: Geophysical Research Letters, v. 28, p. 4267–4270.
Strom, R.G., Schaber, G.G., and Dawson, D.D., 1994, The global resurfacing of Venus: Journal of Geophysical Research, v. 99, p. 10,899–10,926.
Sukhanov, A.L., 1992, Tesserae, *in* Barsukov, V.L., and others, eds., Venus geology, geochemistry, and geophysics: Tucson, University of Arizona Press, p. 82–95.
Sukhanov, A.L., and Pronin, A.A., 1988, Ridged belts on Venus as extensional structures, *in* Lunar and Planetary Science Conference, 29th, March 16–20, 1988: Houston, Tex., Lunar and Planetary Institute, p. 335–348.
Sukhanov, A.L., Pronin, A.A., Burba, G.A., and 9 others, 1989, Geomorphic/geological map of part of the northern hemisphere of Venus: U.S. Geological Survey Miscellaneous Investigations Series Map I–2059, scale 1:15,000,000.
Tanaka, K.L., comp., 1994, Venus geologic mappers' handbook (2nd ed.): U.S. Geological Survey Open-File Report 94–438, 50 p.
Tyler, G.L., Simpson, R.A., Maurer, M.J., and Holmann, E., 1992, Scattering properties of the venusian surface—Preliminary results from Magellan: Journal of Geophysical Research, v. 97, p. 13,115–13,140.
Wilhelms, D.E., 1990, Geologic mapping, *in* Greeley, Ronald, and Batson R.M., eds., Planetary mapping: New York, Cambridge University Press, p. 208–260.
Young, D.A., and Hansen, V.L., 2005, Poludnitsa Dorsa, Venus—History and context of a deformation belt: Journal of Geophysical Research, v. 110, (doc. no.: E03001, doi: 10.1029/2004JE002280).
Zuber, M.T., 1987, Constraints on the lithospheric structure of Venus from mechanical models and tectonic surface features: Journal of Geophysical Research, v. 92, p. E541–E551.

Table 1. *List of volcanic and volcano-tectonic centers in the Meskhent Tessera quadrangle (V–3), Venus (modified from Crumpler and Aubele, 2000).*

Feature name (if named)	Latitude (deg)	Longitude (deg)	Dimension (km)
	Large Volcanoes		
Melia Mons	63	120	300
Amra Tholus	53	98	150
	Coronae		
Tusholi Corona	70	100	150x350
Ops Corona	69	88	100
Fakahotu Corona	60	108	600
	Novae		
—	63.5	90	200
	Calderas		
Anning Paterae	66.55	60	60
—	60.5	83	40x50
Boadicea Paterae	57	95	75–80
—	52.5	96.5	75
	Steep-sided domes		
—	73	100	25
—	70.5	97	30
—	61	83	30
—	57	85	20
—	51.5	104	25
—	51.5	103.5	40
—	51	102.5	45
—	50	97.5	25

Table 2. *List of impact craters within the Meskhent Tessera quadrangle (V–3), Venus (modified from Schaber and others, 1998).*

Crater name	Latitude (deg)	Longitude (deg)	Diameter (km)	Units, crater superposed onto	Lower stratigraphic limit
Esmeralda	64.435	104.516	9.8	pdl/psh	psh
Faina	71.121	100.727	10	gb	gb
Fedorets	59.667	65.594	57.6	pr/ rp_1	rp_1
Firuza	51.8	108.0	6	psh/rp_1	rp_1
Gloria	68.498	94.194	20.7	rp_1	rp_1
Jadwiga	68.387	91.094	12.7	rp_1	rp_1
La Fayette	70.194	107.614	39.6	rp_1	rp_1
Marysya	53.3	75.1	6.3	gb	gb
Masha	60.709	88.553	64.	gb/psh/rp_1	rp_1
Miovasu	72.12	99.951	4.5	rp_1	rp_1
Undset	61.65	60.8	20	pr/gb/psh	psh
Wharton	55.656	61.898	50.4	pr/psh	psh

Table 3. *Area of units mapped in the Meskhent Tessera quadrangle (V–3), Venus.*

Unit label	Area (km^2)	Area (%)
cf	6,000	0.1
c	17,000	0.2
pl	159,000	2.1
ps	138,000	1.8
sc	8,000	0.1
rp_2	256,000	3.3
rp_1	2,116,000	27.6
psh	2,430,000	31.7
pr	351,000	4.6
pdl	186,000	2.4
t	1,081,000	14.1
gb	910,000	11.9
no data	5,000	0.1
TOTAL	7,663,000	100